LINEAR REDUCED ORDER MODELLING FOR GUST RESPONSE ANALYSIS USING THE DLR–TAU CODE

S. Timme[1], K. J. Badcock[1], and A. Da Ronch[2]

[1]School of Engineering, University of Liverpool
Liverpool L63 3GH, United Kingdom
Sebastian.Timme@liverpool.ac.uk

[2]Faculty of Engineering and the Environment, University of Southampton
Southampton SO17 1BJ, United Kingdom

Keywords: Computational Fluid Dynamics, Eigenmodes, Aeroelastic Reduced Order Model, Gust Response, Flutter, DLR–TAU Code

Abstract: A unified modelling approach, using computational fluid dynamics, to calculate the flutter stability and dynamic gust response of realistic aircraft models is outlined. The approach uses an eigenmode decomposition of the coupled problem combined with a (linear or nonlinear) Taylor expansion of the nonlinear, full order residual function. The necessary information for the flutter stability analysis, aerodynamic influence coefficients, is readily calculated. The aerodynamic influence is presented in a form which is in line with industrial practice using corrected doublet lattice method aerodynamics. Based on the stability analysis, eigenmodes are used to produce a reduced model for the gust response analysis. With the projection of the full order system on the eigenmode basis, a small set of equations governing the dominant dynamics is found. The approach is general to work with a variety of numerical schemes for the different physics involved in the coupled problem. In addition, arbitrary parameter variations can be included in the reduced model. The methods are used herein for the computational fluid dynamics solver DLR–TAU, which is adopted by industry throughout Europe, for aerodynamics. Structures are described by the standard modal form of a finite–element model. While pre–computations to evaluate the reduced order model require heavy computational resources, the reduced model can be solved in a matter of seconds on a desktop machine. The test cases presented to demonstrate the modelling capability include a wing structure and a realistic passenger aircraft.

1 INTRODUCTION

This paper presents the details of a combined modelling approach to be used both for flutter stability and dynamic gust response analyses of realistic aircraft configurations. Aerodynamics are modelled with computational fluid dynamics (CFD) and the widely used DLR–TAU code is chosen for this. The reduced order model for gust response simulations builds on previous developments done for flutter stability analysis with linearised frequency domain CFD aerodynamics.

Early work to predict the stability behaviour of an aircraft structure attempted to solve the coupled problem of linearised CFD aerodynamics and modal structures for the instability point directly [1]. Later, to gain understanding of the behaviour of the aeroelastic modes with dynamic pressure, shift–and–invert methods were used [2]. It was soon realised that the Schur complement of the coupled Jacobian matrix offers computational advantages [3]. Still, the Schur formulation and its different approximations were deemed too costly for

routine analysis as many operations on the full order aerodynamics are required, and a surrogate aerodynamics model based on interpolation, as in classical doublet lattice method (DLM) analysis, was introduced [4]. The body of work has been summarised in [5].

Concerning the eigenmode model reduction, early work discussed that the system dynamics are dominated by the critical mode, and this centre manifold reduction was applied to transonic aeroelastic limit cycle response and also its sensitivity to parametric variation [2, 6]. Recently, the method was extended to deal with multiple modes and applied to dynamic gust response analysis and control design [7–9].

In Section 2 the theory of the modelling approach for stability and response analyses is outlined, while details of the numerical implementation are given in Section 3. Results for two test cases, including a wing and a passenger aircraft, are provided in Section 4 to demonstrate the prediction capability of the approach presented.

2 THEORETICAL FORMULATION

The coupled equations of fluid and structure can be written in a first order semi–discrete form as

$$\dot{w} = \boldsymbol{R}(\boldsymbol{w}, \boldsymbol{\theta}) \tag{1}$$

where the vectors of unknowns $\boldsymbol{w}$ and corresponding, highly nonlinear, residuals $\boldsymbol{R}$ contain both the fluid and structural contributions. The dimension of the problem is n. The system also depends on a set of chosen system parameters described by $\boldsymbol{\theta}$. We introduce a deviation $\Delta\boldsymbol{w}$ of the coupled solution around an equilibrium point $\boldsymbol{w}_0$ as

$$\Delta\boldsymbol{w} = \boldsymbol{w} - \boldsymbol{w}_0 \tag{2}$$

and furthermore linearise the dynamics at this equilibrium point which results in the right eigenvalue problem

$$A\Phi = \Phi\Lambda \tag{3}$$

where $A = \frac{\partial \boldsymbol{R}}{\partial \boldsymbol{w}}$ is the Jacobian matrix built from four significant blocks representing the dependencies between fluid and structure. The matrix Λ is diagonal containing the eigenvalues λ^j, while Φ is a matrix formed by the right eigenvectors $\boldsymbol{\phi}^j$ as its columns. Similarly, the corresponding left eigenvalue problem is given by

$$\Psi^H A = \Lambda\Psi^H \tag{4}$$

where the matrix Ψ contains the left eigenvectors $\boldsymbol{\psi}^j$ as columns, and Ψ^H is the conjugate transpose (Hermitian) matrix of Ψ. An appropriate normalisation of the right and left eigenvectors will satisfy the biorthonormality conditions

$$\Psi^H \Phi = I \quad \text{and} \quad \Psi^H \bar{\Phi} = O \tag{5}$$

with I as identity matrix and O as a zero matrix. The expression $\bar{\Phi}$ denotes the complex conjugate of Φ. The relations

$$\Psi^H A \Phi = \Lambda \quad \text{and} \quad \Psi^H A \bar{\Phi} = O \tag{6}$$

apply accordingly.

While there are n eigenvalues and corresponding right and left eigenvectors for the coupled problem, a number m with $m \ll n$ is usually sufficient to represent the dominant dynamics of the system. In the current study these m relevant eigenmodes originate in the uncoupled structural system represented in its modal form.

Based on these preliminaries, the methods used for stability and response analyses as well as their close connection from a numerical point of view using CFD to model the aerodynamics are discussed next.

Method for Flutter Stability Analysis

While it is possible to solve the coupled eigenvalue problem in Eq. (3) for the m relevant modes directly in order to trace the eigenvalues with varying dynamic pressure to establish the stability characteristics [2], it is not convenient for models of realistic size. First, simplifications of the coupled system can be made to ease the computational cost and increase robustness [3]. More importantly though, it is advantageous to reformulate the system with CFD aerodynamics in a way to resemble conventional industrial processes with linear aerodynamics (e.g. DLM) for stability analysis [4].

The structural equations of motion in modal form are written as

$$\ddot{\boldsymbol{\eta}} + C_\eta \dot{\boldsymbol{\eta}} + K_\eta \boldsymbol{\eta} = \Xi^T \boldsymbol{f}_a \tag{7}$$

where $\boldsymbol{\eta}$ contains the m modal amplitudes, Ξ is the matrix with 'mass normalised' structural mode shapes as columns, while K_η and C_η are the modal stiffness and damping matrices, respectively. The aerodynamic forces are given by $\boldsymbol{f}_a$, while pre–multiplication with Ξ^T provides the generalised forces. The equations are transformed into first order form. The aeroelastic modes are then traced with changing values of the altitude in a matched–point analysis solving the small nonlinear eigenvalue problem

$$\left(\begin{bmatrix} O & I \\ -K_\eta & -C_\eta \end{bmatrix} + \begin{bmatrix} O & O \\ Q(\omega^j) & O \end{bmatrix} \right) \boldsymbol{\phi}_s^j = \lambda^j \boldsymbol{\phi}_s^j, \qquad j = 1, \ldots, m \tag{8}$$

for the right eigenpair $(\lambda^j, \boldsymbol{\phi}_s^j)$ where $\boldsymbol{\phi}_s^j$ denotes the structural part of the eigenvector $\boldsymbol{\phi}^j$. Also, the connection between the generalised forces $\Xi^T \boldsymbol{f}_a$ and the modal amplitudes $\boldsymbol{\eta}$ through the matrix Q is clear. The nonlinearity in the latter equation is due to the dependence of the aerodynamics contained in the matrix Q on the eigenvalue λ^j. The circular frequency ω^j is the imaginary part of the eigenvalue λ^j.

The aerodynamic influence $Q(\omega)$ is modelled here with CFD using linear frequency domain functionality to evaluate linear systems

$$(A_{ff} - i\omega I)Y = -A_{f\eta} - i\omega A_{f\dot{\eta}} \tag{9}$$

with the subscripts of A indicating the fluid and structural contributions of the coupled Jacobian matrix. The solution $Y \in \mathbb{C}^{n_f \times m}$ with n_f as number of fluid unknowns is then integrated over the aerodynamic surface of the aircraft or wing structure,

$$Q(\omega) = A_{\dot{\eta}f} Y \tag{10}$$

to form matrix $Q \in \mathbb{C}^{m \times m}$. While it is straightforward using CFD to evaluate the aerodynamic response to a modal excitation with complex frequency, we restrict the discussion here to simple harmonic motion as usually done in industrial practice.

Note that the right–hand side of Eq. (9) follows from the underlying assumption of the linearisation when converting the structural ordinary differential equations from second to first order form, i.e. $\dot{\phi}_\eta = \lambda\phi_\eta$ and $\phi_s = [\phi_\eta^T, \lambda\phi_\eta^T]^T$. Also observe matrix $A_{\eta f}$ is zero due to this first order form of the structural equations. Evaluating matrix $A_{\dot{\eta}f}$ on the other hand is straightforward as it basically involves multiplication of the structural mode shape matrix Ξ with aerodynamic surface normal vectors while taking care of the transformation between conservative and primitive variables in the fluid equations.

Solving Eq. (9) repeatedly while tracing the aeroelastic eigenvalues is too expensive and simplifications are introduced. Similar to industrial processes, the matrix Q is pre–computed for different parameter combinations and then interpolated. In the current study we apply the method of kriging for the task of interpolation [4], while other multi-dimensional interpolation tools can be used.

Method for Dynamic Gust Analysis

The reduced order model for dynamic gust response analysis is an extension of the method used for stability analysis in that the eigenvalues and eigenvectors of the aeroelastic system are used in an eigenmode reduction of the full order system. The model reduction approach is outlined below with more details to be found in [7].

The nonlinear residual vector $\boldsymbol{R}(\boldsymbol{w}, \boldsymbol{\theta})$ in Eq. (1) is expanded about the steady state solution $\boldsymbol{w}_0$ and a specified set of system parameters $\boldsymbol{\theta}_0$ as follows

$$\Delta\dot{\boldsymbol{w}} = \boldsymbol{R}(\boldsymbol{w}_0, \boldsymbol{\theta}_0) + A\Delta\boldsymbol{w} + \frac{1}{2!}B(\Delta\boldsymbol{w}, \Delta\boldsymbol{w}) + \frac{1}{3!}C(\Delta\boldsymbol{w}, \Delta\boldsymbol{w}, \Delta\boldsymbol{w}) + \frac{\partial\boldsymbol{R}}{\partial\boldsymbol{\theta}}\Delta\boldsymbol{\theta} + \dots \quad (11)$$

to form a nonlinear ordinary differential equation for the variation $\Delta\boldsymbol{w}$. Dots indicate all other inessential terms. The residual $\boldsymbol{R}(\boldsymbol{w}_0, \boldsymbol{\theta}_0)$ at the steady state is zero while the last term describes the influence of parameters on the dynamics. A higher order expansion with respect to a parameter variation is possible as well. Higher order terms in the Taylor expansion, such as the second and third Jacobian operators, B and C, respectively, are neglected in the current study and are not further discussed. We discuss a linear aeroelastic model reduction.

The deviation $\Delta\boldsymbol{w}$ from the steady state solution $\boldsymbol{w}_0$ is evaluated using a transformation of variables

$$\Delta\boldsymbol{w} = \Phi\boldsymbol{z} + \bar{\Phi}\bar{\boldsymbol{z}} \quad (12)$$

where $\boldsymbol{z} \in \mathbb{C}^m$. This transformation of variables basically describes $\Delta\boldsymbol{w}$ as a linear combination of the (complex–valued) aeroelastic mode shapes $\Phi \in \mathbb{C}^{n\times m}$.

Following substitution and pre–multiplication with the conjugate transpose of the left modal matrix Ψ, the full order system simplifies to

$$\dot{\boldsymbol{z}} = \Lambda\boldsymbol{z} + \Psi^H\frac{\partial\boldsymbol{R}}{\partial\boldsymbol{\theta}}\Delta\boldsymbol{\theta} \quad (13)$$

where the biorthonormality conditions from Eq. (5) are applied. This establishes a very small system which can easily be integrated in time. Note that the term $\Psi^H\frac{\partial\boldsymbol{R}}{\partial\boldsymbol{\theta}}$ for parameter variation can be evaluated once and stored initially, thus adding little to the computing requirements when solving for $\boldsymbol{z}$.

Some more discussion of the last term in the latter equation is needed. The model reduction is general to deal with arbitrary parameter variations, which makes it possible to be used in design tasks. Specifically for the gust response problem, the parameter vector $\boldsymbol{\theta}$ constitutes the components of the spatially and temporally varying gust velocity field $\boldsymbol{v}_g(\boldsymbol{x}, t)$. Arbitrary gust shapes, discrete and continuous, can be considered. More insight in dealing with this gust disturbance influence term is provided in the next sections.

3 NUMERICAL ASPECTS

In the current work we make full use of functionality available in the DLR–TAU code to evaluate the aerodynamics in the coupled problem based on CFD. To ease the computational cost associated with using CFD, an approach similar to standard (i.e. linear aerodynamics) methods is followed for the flutter problem. The aerodynamic influence is evaluated initially at a small number of points in a parameter space defined by reduced frequency and Mach number. An interpolation surrogate model, based on the pre–computed aerodynamics, is then employed when solving the aeroelastic stability problem at negligible further cost.

In terms of the model reduction for gust response prediction, the flutter method provides the eigenvalues λ^j and corresponding structural part of the right eigenvectors $\boldsymbol{\phi}_s^j$ of the aeroelastic system at a chosen subcritical altitude. Accordingly the left eigensolution for the structural part $(\lambda^j, \boldsymbol{\psi}_s^j)$ can be found by solving the adjoint problem of Eq. (8)

$$\left(\begin{bmatrix} O & I \\ -K_\eta & -C_\eta \end{bmatrix} + \begin{bmatrix} O & O \\ Q_\eta & Q_{\dot{\eta}} \end{bmatrix} \right)^T \bar{\boldsymbol{\psi}}_s^j = \lambda^j \bar{\boldsymbol{\psi}}_s^j, \qquad j = 1, \ldots, m \tag{14}$$

where the subscripts of matrix Q now indicate the aerodynamic derivatives due to modal deflection and velocity, respectively. While for the right structural eigenvector the relation $\dot{\boldsymbol{\phi}}_\eta = \lambda \boldsymbol{\phi}_\eta$ is obvious, the same relation does not apply for the left eigenvector. As a consequence the right–hand side of Eq. (9) to evaluate the aerodynamic influence Q does not apply for the left eigenvalue problem either and, in general, twice the number of linear systems per evaluation of an appropriate $\widetilde{Q} = [Q_\eta, Q_{\dot{\eta}}]$ have to be solved with the right–hand side $A_{fs} = [A_{f\eta}, A_{f\dot{\eta}}]$.

To avoid the doubling of cost for the precursor flutter analysis, the generation of the aerodynamic influence could be modified by a simple trick to solve

$$\widetilde{Q}(\omega) = -\left(A_{fs}^T (A_{ff}^T - i\omega I)^{-1} A_{\dot{\eta}f}^T \right)^T \tag{15}$$

instead requiring m linear solves per matrix $\widetilde{Q}$ just as above for Q, while being general to be applied equally to right and left structural eigensolutions.

Based on the information for right and left structural eigensolutions, the fluid parts of the eigenvectors are obtained again using the linear frequency domain functionality within the DLR–TAU solver. The equation to evaluate the right fluid eigenvectors follows from rearranging the coupled system in Eq. (3) for the fluid part,

$$\begin{aligned} (A_{ff} - \lambda^j I)\boldsymbol{\phi}_f^j &= -A_{fs}\boldsymbol{\phi}_s^j \\ &= -A_{f\eta}\boldsymbol{\phi}_\eta^j - A_{f\dot{\eta}}\dot{\boldsymbol{\phi}}_\eta^j, \qquad j = 1, \ldots, m \end{aligned} \tag{16}$$

where m linear system solves are required. The corresponding equation to compute the left fluid eigenvectors can be derived from the adjoint problem of the coupled system,

$$
\begin{aligned}
(A_{ff}^T - \bar{\lambda}^j I)\boldsymbol{\psi}_f^j &= -A_{sf}^T \boldsymbol{\psi}_s^j \\
&= -A_{\dot{\eta}f}^T \dot{\boldsymbol{\psi}}_\eta^j, \qquad j = 1, \ldots, m
\end{aligned}
\tag{17}
$$

adding another m linear solves to the cost per eigenmode basis.

It is noted however that the fluid part of the eigenvectors could be evaluated without solving linear systems altogether. A right fluid eigenvector, for instance, basically is a linear combination of the aerodynamic responses due to modal excitation weighted by the structural eigenvector components. When calculating the samples of the aerodynamic matrix Q for the flutter analysis, linear systems of the form as shown in Eq. (9) are solved. A good approximation for the right eigenvectors would be interpolation of the linear frequency domain solution between frequencies while setting the damping value to zero. When working with $\widetilde{Q}$ from Eq. (15) instead, a similar argument applies for the left eigenvectors. In the current work the eigenvectors are found by explicitly solving the linear systems in Eqs. (16) and (17).

To model the influence of an arbitrary gust input on the dynamics in the reduced model, the last term in Eq. (13) needs to be pre–computed. In the current study the field velocity approach [10] is used, where a gust disturbance is introduced through modifying the point velocities of the computational mesh. The gust disturbance is assumed to be frozen and not influenced by the structural response. The approach is widely used and considered to give small differences for gust lengths of practical importance when compared to modelling the non–frozen gust disturbance through a farfield boundary condition, for instance.

Different levels of approximation to model the gust input, which is always a function of time, based on the field velocity approach are possible. At the lowest level of approximation we would discuss the gust input as a three parameter problem for the three components of the gust velocity ignoring spatial variation altogether. At the highest level of approximation we deal with a $3n_p$ parameter problem where n_p is the number of grid points allowing for spatial variation throughout the computational domain.

Using the DLR–TAU code, the gust term for the former approximation is evaluated using finite differences, e.g. for a vertical gust

$$
\frac{\partial \boldsymbol{R}}{\partial w_g} = \frac{\boldsymbol{R}(\dot{\boldsymbol{x}}^{(z)} + \epsilon) - \boldsymbol{R}(\dot{\boldsymbol{x}}^{(z)} - \epsilon)}{2\epsilon}
\tag{18}
$$

where $\dot{\boldsymbol{x}}^{(z)}$ is the mesh velocity in the vertical direction and w_g is the corresponding component of $\boldsymbol{v}_g(t) \in \mathbb{R}^3$. Note that the mesh velocity is disturbed throughout the computational domain at once thus only providing a variation in the gust input with respect to time but not space. The required reduced model coefficients of dimension $\mathbb{C}^{m \times 3}$ are pre–computed from the matrix product $\Psi^H \frac{\partial \boldsymbol{R}}{\partial \boldsymbol{v}_g}$. This method to model the gust disturbance in the reduced model is referred to as 'vector' approach hereafter.

The most general approximation, referred to as 'matrix' approach, is to evaluate the Jacobian matrix of the fluid residual with respect to the mesh velocity allowing for spatial

	Grid size	MG3w	ILU(0)	ILU(1)
unstructured	225k	0.8	2.0	3.9
structured	400k	1.1	1.9	2.7
structured	740k	2.0	3.5	5.0

Table 1: Memory requirements per core in gigabyte for GMRes linear solver with different preconditioners (using 100 Krylov vectors and running on 4 cores).

variation in the gust input with $\boldsymbol{v}_g(\boldsymbol{x}, t) \in \mathbb{R}^{3n_p}$. The required model coefficients of dimension $\mathbb{C}^{m \times 3n_p}$ are pre–computed in the same way as for the 'vector' approach. Using this alternative method, the gust input $\Delta \boldsymbol{v}_g(\boldsymbol{x}, t)$ basically becomes a binary vector amplified by the local value of the gust velocity (gust shape dependent) which can easily be formed knowing the location of the grid points in the reduced model.

In the current work both the 'vector' and the 'matrix' approach are used to model the influence of the gust input in the reduced model. For the 'matrix' approach, the Jacobian matrix of the fluid residual with respect to the mesh velocity is evaluated in a brute force fashion using finite differences as an analytical formulation is currently missing.

Solving Linear Systems

To solve the large sparse linear systems of the general form $A\boldsymbol{x} = \boldsymbol{b}$ we use the preconditioned restarted generalized minimal residual (GMRes) method [11]. Preconditioning is provided using a block incomplete lower upper (ILU) factorisation of an approximation to the coefficient matrix A with variable level of fill–in. The coefficient matrix for the factorisation is based on a linear combination of Jacobian matrices from first and second order spatial discretisations [12]. Complex arithmetic is used which removes the requirement of augmenting to form an equivalent real–valued problem of twice the size. Fill–in during the factorisation is possible, while retaining the original sparsity for zero fill–in is usually sufficient for acceptable convergence rates.

The ILU–GMRes option has higher memory requirements compared with the standard GMRes option available within the DLR–TAU code using multigrid (MG) for preconditioning. However, ILU preconditioning outperforms MG significantly both in terms of computing time and convergence rates. While the ILU factorisation has an one–off cost, several MG cycles are required at each iteration step. The MG approach fails to reach convergence levels similar to ILU, despite additional simplification in the fluid equations such as frozen turbulence. While the examples in the current paper assume inviscid flow solving the Euler equations, in unpublished studies a similar behaviour was observed for viscous flow solving the Reynolds–averaged Navier–Stokes equations with a suitable turbulence model.

Table 1 shows the approximate memory requirements while solving linear systems for typical computational grids from CENTAUR (unstructured) and ANSYS ICEM CFD (block–structured), respectively. For the ILU(k) preconditioners, where k denotes the level of fill–in, the coefficient matrix is based on a combination of first and second order schemes maintaining a second order sparsity. The MG approach uses a 3w cycle. The data in the table indicate that, depending on the problem, six to eight gigabyte of memory per core are usually sufficient and practical using incomplete factorisations for preconditioning to accommodate up to 200,000 grid points.

7

(a) Goland wing – mode 2   (b) XRF1 aircraft – mode 1

Figure 1: Aerodynamic surfaces of test cases including representative projected mode shapes.

Computational Cost

After the nonlinear steady state solution is calculated, solving the large sparse linear systems is the main cost in any approach adopting linear frequency domain functionality. The current approach for flutter analysis relies on sampling the multidimensional parameter space. Thus, the cost per reference Mach number (and angle of attack, trim conditions, mass case, etc.) scales with the number m of modes retained (typically 20 to 100) times the number of reduced frequencies considered (typically less than ten).

In addition, per basis for model reduction to analyse the gust response an additional $2m$ linear solves are required, which could be reduced to m by an appropriate interpolation of solutions obtained while calculating samples for the precursor flutter analysis. The evaluation of the terms to include the influence of parameters on the dynamics is relatively cheap as it can be done using finite differences in the absence of an analytical formulation. Automatic differentiation could also be considered as an alternative.

4 RESULTS

Results are presented for two test cases. The Goland wing is rectangular and cantilevered with a constant cross section of a symmetric, 4% thick, parabolic–arc aerofoil and rounded wing tip. It has a chord length of 6 ft and a span of 20 ft. The computational mesh for the Euler CFD calculations has about 400,000 points. The structural model is that for the wing/store configuration as described in [13]. Four normal modes are retained, while structural damping is ignored. The second mode (i.e. torsion) as mapped to the CFD surface mesh is shown in Fig. 1. Note that the aerodynamics of the tip store are not modelled.

The aircraft model XRF1 has dimensions of a wide–body passenger aircraft with a semi–span of about 30 m and an overall length of about 65 m. The computational mesh for the Euler CFD calculations has about 740,000 points. Fifteen normal modes are retained with structural damping ignored. The first mode, dominant in wing bending, as mapped to the CFD surface mesh is illustrated in Fig. 1.
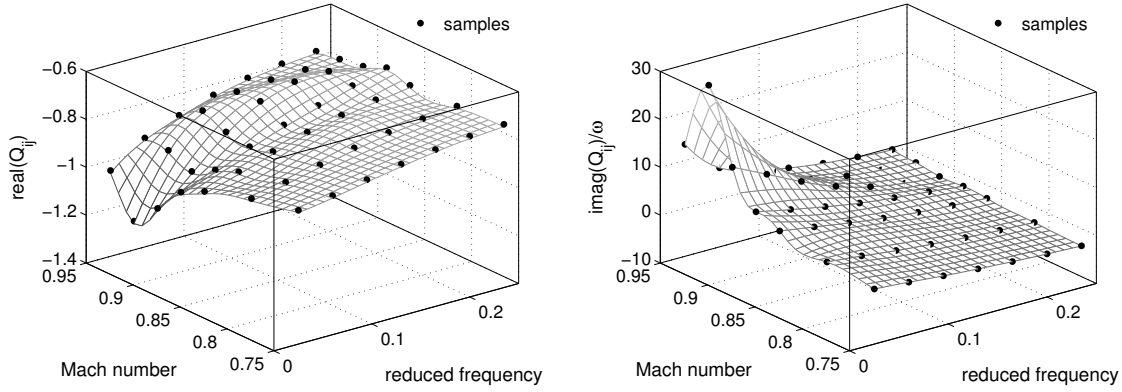
Figure 2: Representative element of aerodynamic influence matrix (real and imaginary part) for baseline Goland wing/store configuration using Euler flow model.
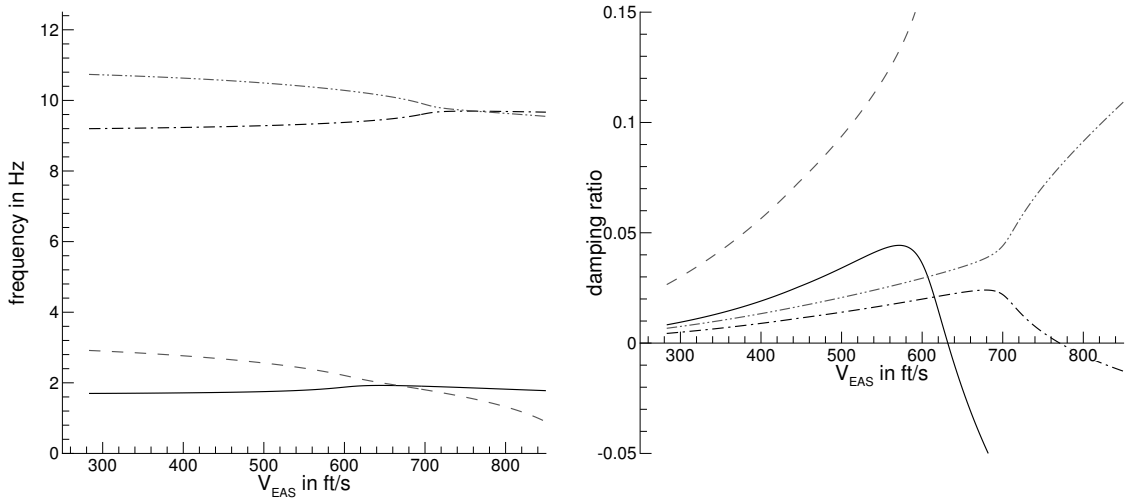
Figure 3: Frequency and damping ratio for four modes of baseline Goland wing/store configuration as function of equivalent airspeed at Mach 0.845.

One representative element of the aerodynamics matrix Q for the Goland wing/store configuration is shown in Fig. 2. The element describes the relation between the aerodynamic response in the first degree–of–freedom due to changes in the second generalised coordinate. The black dots in the figure indicate sample locations while the meshed surfaces represent the kriging interpolation used in the stability analysis to describe the variation of the matrix elements. The two dimensional parameter space is defined by the reduced frequency and freestream Mach number. Note that the reduced frequency is the primary parameter dimension which always has to be included in the sampling as the eigenvalue problem is nonlinear. Solving the eigenvalue problem gives a prediction of the eigenvalue and structural eigenvector for a given dynamic pressure, where the eigenvalue is used itself to define the parameter space for the sampling of the matrix Q. From the figure it can be seen that CFD aerodynamics are needed in the transonic range, while at lower Mach numbers a linear potential aerodynamics theory would be sufficient.

An example of such a flutter analysis is given in Fig. 3 for the Goland wing/store configuration. The frequency and damping ratio of the four modes are shown as a function of the equivalent airspeed V_{EAS}. The configuration encounters a dynamic instability at

9
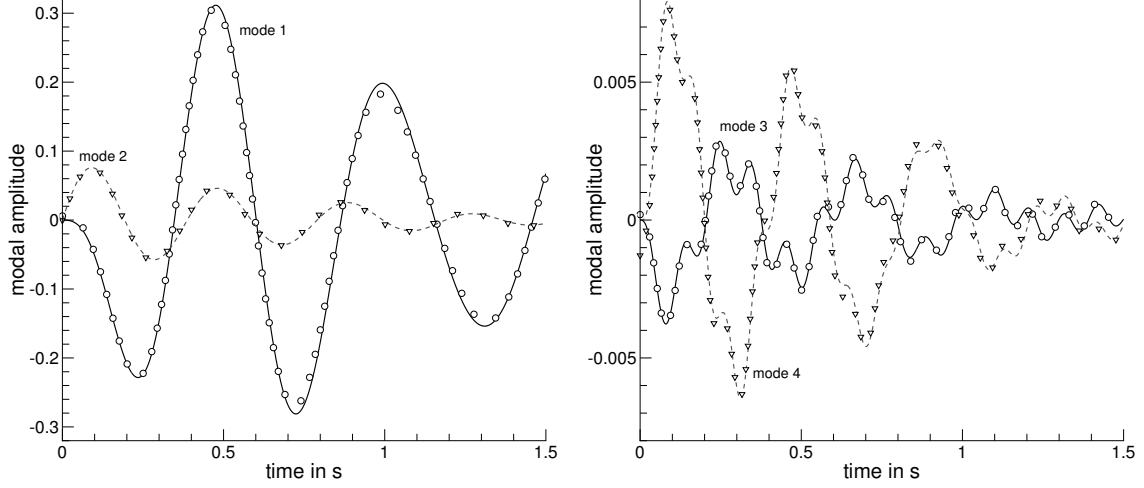
Figure 4: Free response of Goland wing/store configuration to initial disturbance at Mach 0.845 and altitude of 30,000 ft; lines are full order reference solution, while symbols are results from reduced model.

about 630 ft/s equivalent airspeed (corresponding to about 20,580 ft altitude) following the typical bending–torsion coupling in the two lowest frequency modes.

Following this precursor flutter analysis, a subcritical altitude of 30,000 ft (about 514 ft/s equivalent airspeed) is chosen for exercising the reduced order model for gust response analysis. Figure 4 demonstrates the quality of the computed eigenmode basis. Here the response of the system to an initial disturbance in the modal velocity of the second mode is illustrated. The differences between the full order reference solution and the model reduction results are small building confidence in the model reduction. Also the two higher frequency modes are predicted accurately having an amplitude two orders of magnitude smaller than the first mode. The results from the reduced model are obtained in much less than a second of computing time on a desktop computer compared with many hours to simulate the reference solution.

As said above, both the 'vector' and the 'matrix' approach are discussed to model the gust disturbance using the field velocity approach. In either case a discrete '1-cosine' gust profile in the vertical direction with different gust lengths is chosen, while arbitrary gust shapes are possible as well. For the 'vector' approach, the spatially constant, vertical gust velocity $w_g(t)$ is modelled as

$$ w_g(t) = \tfrac{1}{2} w_{g0} \Big(1 - \cos \big(\tfrac{2\pi}{T_g}(t - t_0) \big) \Big), \qquad t_0 \le t \le (t_0 + T_g) \tag{19} $$

where $L_g = V_{\text{TAS}} T_g$ with L_g as the gust length and T_g as corresponding period. The velocity V_{TAS} denotes the true airspeed. The time t_0 is the duration of time before the aircraft structure penetrates the gusty field, while w_{g0} is the gust intensity. Accordingly, in the 'matrix' approach we use

$$ \boldsymbol{w}_g(\boldsymbol{x}, t) = \tfrac{1}{2} w_{g0} \Big(1 - \cos \big(\tfrac{2\pi}{L_g}(\boldsymbol{x} - V_{\text{TAS}}(t - t_0) + L_g) \big) \Big), \\ V_{\text{TAS}}(t - t_0) - L_g \le \boldsymbol{x} \le V_{\text{TAS}}(t - t_0) \tag{20} $$

to model the vertical gust disturbance field, which, in contrast to the 'vector' approach, describes a travelling (spatially and temporally varying) gust. It should be clear that the latter approach is more general and realistic.

10
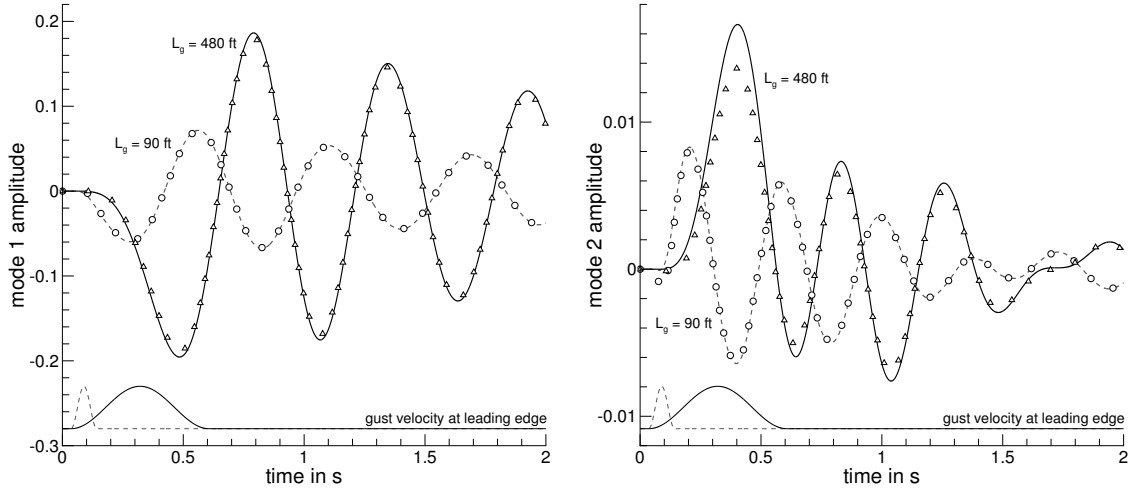
Figure 5: Response of Goland wing/store configuration to '1-cosine' gust at Mach 0.845 and altitude of 30,000 ft; lines are full order reference solution, while symbols are results from reduced model.
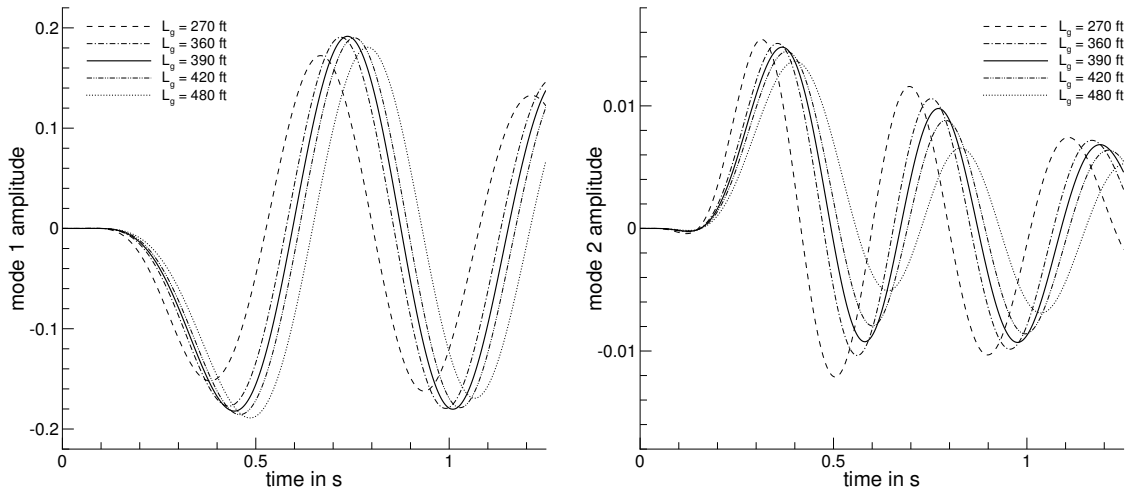
Figure 6: Identifying worst case gust length for Goland wing/store configuration to '1-cosine' gust at Mach 0.845 and altitude of 30,000 ft using reduced order model.

Figure 5 presents the gust response in the first and second mode to the '1-cosine' gust input at two different gust lengths. The two gust lengths are tuned to the first and third mode frequencies, respectively. The gust shape (not to scale) is included in the lower part of the figures to indicate the relation with the vibration frequency. The 'vector' approach is used for the results in the figures, while it was found in the case of the Goland wing that the differences compared with the 'matrix' approach are insignificant and thus not shown. This has two reasons. First, the gust lengths considered (based on the normal mode frequencies) are large with 10 to 100 times the chord length. Secondly, the Goland wing is unswept and effects due to gradual chordwise gust entry along the span are not relevant.

Figure 6 explores the application of the reduced model to search for the worst case gust length at the chosen flight conditions in terms of maximum modal deflections. With little surprise, the gust lengths tuned to the normal mode frequencies cause the highest amplitudes in the respective modes. Note that the gust intensity used was held constant and

11
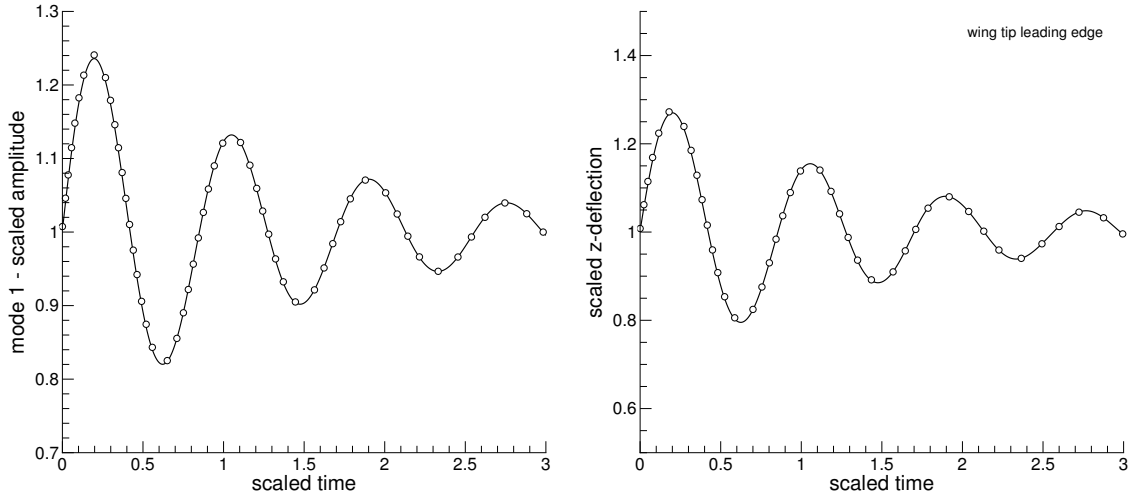
Figure 7: Free response of passenger aircraft to initial disturbance at Mach 0.85 and altitude of 12,000 m; lines are full order reference solution, while symbols are results from reduced model.

not, as described, for instance, in [14], related to the gust length. As before, the 'vector' approach is used. The reduced model simulations at different gust lengths taken together require about one second, while the 'matrix' approach is about 100 times more expensive (yet significantly less expensive than a single full order simulation). The higher cost of the 'matrix' approach is due to the requirement to repeatedly evaluate the gust velocity at all points of the original computational mesh and pre–multiplying this vector with the pre–processed model coefficients $\Psi^H \frac{\partial \boldsymbol{R}}{\partial \boldsymbol{v}_g}$ when solving for $\boldsymbol{z}$. It should be emphasised however that we are essentially solving a parametric problem with n_p independent parameters (considering only vertical gust disturbance).

Results for the second test case are presented in Figs. 7 and 8. Figure 7 gives the free response of the system to an initial disturbance in the modal velocity of the first mode. The flight conditions describe a subcritical altitude of 12,000 m and a Mach number of 0.85 with one degree angle of attack resulting in a strong shock wave. Static aeroelastic deformation is fully accounted for. Both the amplitude of the (dominant) first mode and the physical deflection of the wing tip leading edge point, summing the contributions from all modes, are shown. Note that the time is scaled by the first mode frequency, while deflections are scaled by the corresponding value of the static aeroelastic deformation. Excellent agreement between the results is observed.

It is important to note that the entire flowfield can be reconstructed as well using Eq. (12), while only modal amplitudes and wing tip deflection are shown herein. Obtaining time histories of pressure distributions, for instance, to evaluate the aerodynamic loading would only require post–processing.

Figure 8 shows the gust response to the '1-cosine' gust input at two different gust lengths. For these gust simulations only the results from the 'matrix' approach are presented. While the response is well predicted once the aircraft moves past the gusty field as can be seen in the figure, there are discrepancies when the aircraft penetrates the gust. This is more pronounced for the longer gust length. A similar, less distinct behaviour is observed above in Fig. 5 for the Goland wing configuration as well. These discrepancies in gust response are not due to the gust intensity used, which is 1% of the true airspeed for the
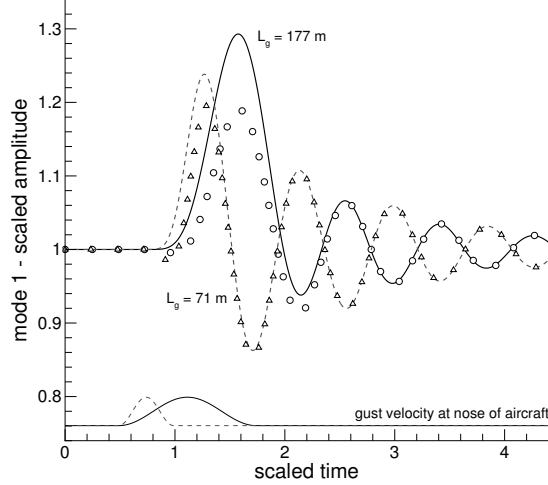
Figure 8: Response of passenger aircraft to '1-cosine' gust at Mach 0.85 and altitude of 12,000 m; lines are full order reference solution, while symbols are results from reduced model using 'matrix' approach.

aircraft simulations. Indeed, simulated lower values of gust intensity simply scale the presented results (and also the error) linearly as the model reduction is linear herein.

There seem to be two possible explanations for the discrepancies between reference and reduced order model results. One is due to the choice of the reduced model basis as previously mentioned in [7]. Therein a typical section aerofoil using linear aerodynamics based on Wagner's and Küssner's functions (to model the lift contributions due to the aerofoil motion and the penetration into a gusty field, respectively) was discussed. A flap was added for control design. Including only the two modes corresponding to the pitch and plunge degrees–of–freedom, the reduced model results were not accurate compared with the full order solution. Adding a third basis vector, with an eigenvalue corresponding to a time constant in the approximation to Küssner's function, improved the prediction clearly independent of the gust length. From a related point of view, a structure experiences a variation in the aerodynamic loading due to a gust disturbance without the structural motion in a static simulation. Thus, the questions arise if there exists, using CFD aerodynamics, a similar universal aerodynamic mode, and how to include such a mode in the reduced order basis effectively.

The other explanation is due to the expansion of the residual function with respect to the parameters $\boldsymbol{\theta}$. Strictly, the solution vector depends on the parameters, and thus the nonlinear system in Eq. (1) is written as $\dot{\boldsymbol{w}} = \boldsymbol{R}\big(\boldsymbol{w}(\boldsymbol{\theta}), \boldsymbol{\theta}\big)$, introducing the term

$$\left(\frac{\partial \boldsymbol{R}}{\partial \boldsymbol{\theta}} + \frac{\partial \boldsymbol{R}}{\partial \boldsymbol{w}} \frac{\partial \boldsymbol{w}}{\partial \boldsymbol{\theta}} \right) \Delta \boldsymbol{\theta}$$

in the expansion in Eq. (11) due to the chain rule. These different points and their contribution to the model reduction need to be better understood and investigated.

5 CONCLUSIONS

This paper presents a unified modelling approach, using computational fluid dynamics, to deal both with flutter stability and dynamic gust response analyses of realistic aircraft

13

problems. The model reduction for the gust response analysis is based on an eigenmode decomposition of the system dynamics and subsequent projection of the full order, non-linear residual function onto this vector space. While calculating the eigenmode basis, the required information for a precursor flutter stability analysis is readily provided. The model reduction is general to deal with arbitrary parameter variations to be used for various design tasks, other than gust response, such as control design. Any synthetic gust model in the time domain, discrete or continuous, can be used. The methods are discussed herein using the computational fluids dynamics solver DLR–TAU for the aerodynamics and a standard modal structural model for structures. The test cases presented include a simple wing model as well as a passenger aircraft configuration.

While the flutter method is mature to be readily transferred into an industrial context, and indeed has been tested on a real–life production aircraft configuration using 100 normal modes and solving the Reynolds–averaged Navier–Stokes equations, the model reduction for gust response analysis still requires a deeper understanding. Specifically for the test cases presented, there is an underprediction of the structural response for gust simulations using the reduced order model. Two possible explanations are offered. Based on previous results using linear aerodynamics, a dominant aerodynamic mode (in addition to the coupled eigenmodes originating in the structural system) seems to be required when forming the reduced model basis for dynamic gust response simulations. Furthermore, the dependence of the solution vector on the gust parameters could be important when expanding the nonlinear residual function.

In addition, the flight dynamics response of the aircraft to the gust encounter can be expected to have a significant impact on the loads. Also, the worst case gust response is one of the main drivers for structural sizing, layout and control, and the worst case can be expected to come along with nonlinear dynamic effects. Thus, important future developments for the modelling approach, which are in progress, are to include both a flight dynamics model and an extension to deal with nonlinear effects.

6 ACKNOWLEDGMENTS

7 REFERENCES

[1] Badcock, K. J., Woodgate, M. A., and Richards, B. E. (2005). Direct aeroelastic bifurcation analysis of a symmetric wing based on Euler equations. *Journal of Aircraft*, 42(3), 731–737.

[2] Woodgate, M. A. and Badcock, K. J. (2007). Fast prediction of transonic aeroelastic stability and limit cycles. *AIAA Journal*, 45(6), 1370–1381.

[3] Badcock, K. J. and Woodgate, M. A. (2010). Bifurcation prediction of large–order aeroelastic models. *AIAA Journal*, 48(6), 1037–1046.

[4] Timme, S., Marques, S., and Badcock, K. J. (2011). Transonic aeroelastic stability analysis using a kriging–based Schur complement formulation. *AIAA Journal*, 49(6), 1202–1213.

[5] Badcock, K. J., Timme, S., Marques, S., et al. (2011). Transonic aeroelastic simulation for envelope searches and uncertainty analysis. *Progress in Aerospace Sciences*, 47(5), 392–423.

[6] Badcock, K. J., Khodaparast, H. H., Timme, S., et al. (2011). Calculating the influence of structural uncertainty on aeroelastic limit cycle response. *AIAA Paper 2011–1741*.

[7] Da Ronch, A., Badcock, K. J., Wang, Y., et al. (2012). Nonlinear model reduction for flexible aircraft control design. *AIAA Paper 2012–4404*.

[8] Da Ronch, A., Tantaroudas, N. D., and Badcock, K. J. (2013). Reduction of nonlinear models for control applications. *AIAA Paper 2013–1491*.

[9] Da Ronch, A., Tantaroudas, N. D., Timme, S., et al. (2013). Model reduction for linear and nonlinear gust loads analysis. *AIAA Paper 2013–1492*.

[10] Sitaraman, J. and Baeder, J. D. (2006). Field velocity approach and geometric conservation law for unsteady flow simulations. *AIAA Journal*, 44(9), 2084–2094.

[11] Saad, Y. and Schultz, M. H. (1986). GMRes: A generalized minimal residual algorithm for solving nonsymmetric linear systems. *SIAM J. Sci. Stat. Comput.*, 7(3), 856–869.

[12] McCracken, A., Da Ronch, A., Timme, S., et al. (2013). Solution of linear systems in Fourier–based methods for aircraft applications. *International Journal of Computational Fluid Dynamics*, 27(2), 79–87.

[13] Beran, P. S., Khot, N. S., Eastep, F. E., et al. (2004). Numerical analysis of store–induced limit–cycle oscillation. *Journal of Aircraft*, 41(6), 1315–1326.

[14] Gust and turbulence loads. *Electronic Code of Federal Regulations (e-CFR)*. Title 14, Part 25.341, Federal Aviation Administration. http://www.ecfr.gov/.